# Charge Polarization and Current Distribution in a Conductive Particle in the Rayleigh Region

Tao Shen, Ming Yan, and Thomas T. Y. Wong

***Abstract*—An investigation of the interaction of a conductive sphere with an electromagnetic wave with attention given to space-charge effects would appear timely, as there is much current interest in the electromagnetic properties of mesoscopic structures. In this study, the polarization of a small semiconductor sphere immersed in a dynamic electric field is explored analytically and numerically. In one approach, suitable for a sphere with low to moderate charge carrier concentration, the Poisson's equation is coupled with the transport equations of the carriers, leading to a quasi-static formulation under the weak-field approximation. Screening effects of the charges on the interior field are revealed, along with a current distribution that is essentially uniform over much of the volume of the sphere. Frequency dependence of the total induced dipole moment of the sphere displays strong dispersion and absorption near the bulk plasma frequency. Validity of the quasi-static assumption is assessed by comparison to results of calculations based on a full-wave formulation. As the nominal carrier concentration exceeds $10^{20}\ cm^{-3}$, the quasi-static solutions for interior field and current distribution begin to deviate from the full-wave solution and the latter must be employed to provide a realistic account of the charge-wave interaction within the sphere.**

***Index Terms*—Conductive materials, current distribution, polarization, Rayleigh scattering, space charge.**

## I. Introduction

RECENT advancements in nanotechnology have led to considerable interest in the study of electromagnetic properties of structures with nanometer length scale [1]–[4]. For activities in the frequency range of interest to antenna engineers, the wavelength is often large compare to the dimensions of these structures. Placed in the perspective of wave scattering, the term Rayleigh scattering may be employed to characterize the interactions. Scattering by the sphere is a subject of fundamental interest that has received much attention over the years [5]–[11], while the solution to the electromagnetic waves within and outside the sphere has been employed to validate newly developed computation methods for electromagnetic fields and wave propagation.

Scattering by a sphere in the Rayleigh region [12] is often accounted for by a quasi-static formulation in which a scalar potential with harmonic time dependence is introduced to provide the solution for the internal and external fields [13]. Elaborate theory for the polarization within spherical particles characterized by different forms of dielectric functions has been developed and successfully applied to account for their scattering properties [14]–[16]. The dielectric functions employed are often based on that of molecular species containing bound charges that would exhibit orientation or displacement polarizations, leading to a relaxation-type of response function [17] or its derivatives. In the presence of mobile charges as in the case of metallic particles, a complex dielectric function based on the bulk conductivity of the material has been employed to account for the absorption peak observed for metallic particles near their bulk plasma frequencies in the optical region. Indeed, an immediate application of the Mie series solution [18] for the sphere when it was arrived at was in explaining the scattering of light by gold particles.

The interaction of particles with an electromagnetic wave has been a subject of interest to antenna engineers, as composite materials containing particles with unique dispersion and absorption properties may be employed to enhance antenna performance in terms of both the radiation pattern and bandwidth. Interest in synthetic materials has been intensified in recent years with the demonstration of antenna properties improvement by metamaterials [19]. At the same time, as the frequency of operation for communication systems continues to increase, atmospheric absorption and scattering become a significant factor in the link budget. Particles in the atmosphere or within a waveguiding structure can have effects on the quality of transmission and must be taken into consideration [20].

The use of bulk parameters for a material can have its limitation when boundary effects are significant. A typical example is the application of a dielectric function based on bulk conductivity to account for the polarization of a conductive particle in the static limit [21]. To overcome this difficulty, one needs to incorporate the effect of charge accumulation and depletion on the surface of the spherical boundary. This can be accomplished by employing a transport formulation [22] to describe the dynamics of the conducting species [23], [24], which can be electrons, holes, ions, or other charged entities in the sphere. The transport formulation allows the charge concentration and the velocity of the charge to be treated as separate variables instead of relying on a local bulk conductivity leading to a local complex permittivity. There is another provision of the

Manuscript received February 16, 2012; revised March 24, 2013; accepted April 06, 2013. Date of publication April 23, 2013; date of current version July 31, 2013.

T. Shen is with the Department of Electrical and Computer Engineering, Illinois Institute of Technology, Chicago, IL 60616 USA and also with the College of Materials Science and Engineering, Kunming University of Science and Technology, Kunming, Yunnan 650093, China (e-mail: tshen1@iit.edu).

M. Yan is with Agilent Technologies, Inc., Thousand Oaks, CA 91360 USA (email: yanming@iit.edu).

T. T. Y. Wong is with the Department of Electrical and Computer Engineering, Illinois Institute of Technology, Chicago, IL 60616 USA (e-mail: twong@ece.iit.edu).

Color versions of one or more of the figures in this paper are available online at http://ieeexplore.ieee.org.

Digital Object Identifier 10.1109/TAP.2013.2259571

transport treatment that is vital to provide a realistic description of the charge-field interaction at the surface or interface of a conductive medium, namely the keeping of the conduction current and the displacement current as interacting but separate variables. This enables separate boundary conditions to be written for the mobile charges and the bound charges. The former cannot have a velocity component normal to the surface [21], [25], while the latter satisfies the usual continuity in the electric displacement at the interface of two dissimilar dielectrics.

In this paper, we present the results of computation and a physically realistic interpretation of the electric polarization, internal field, external field, and current distribution in a conductive sphere immersed in an electric field with large wavelength, employing transport equations to describe the motion of the charge carriers. The assumption of excitation by a uniform electric field for the analysis of scattering by small objects with predominantly electric polarization has often been made [13], [20] and found to be effective as supported by agreement with extensive measurement data [26]. Such a field distribution is an idealized situation that can be provided by a few situations such as in the inner region of a parallel-plate capacitor or at the local maximum of the electric field within a cavity resonator, yet the assumption enables the electric polarization process to be considered independent of the magnetic dipole when the coupling between the two is negligible. This assumption will need to be abandoned when the dimension of the scatterer is large compared to the wavelength in the embedding medium. In this work, we focus on the electric polarization in the spherical particle. The magnetic polarization of the sphere is beyond the scope of this discussion.

While the theoretical framework is based on the transport equations for electrons and holes in a semiconductor, it can also be applied to describe the properties of a spherical particle containing other kind of charges such as ions, when appropriate parameters are substituted in the equations of motion and charge population. While the calculations employed to illustrate the phenomena of interest were performed using parameters typical for doped silicon, the formulation can be applied to other semiconductors. For ionic conductors in which the ionic motion can be accounted for by momentum relaxation, the formulation is also applicable when the appropriate material parameters are employed in the equations. The formulation is also applicable to metal, for which only electrons need to be considered, while a relative permittivity of unity needs to be employed in the equations. Discussions of the metallic particle is not included in this paper because the nature of interaction does not involve lattice polarization, leading to a difference in the frequency dependence of the power absorption peak near the plasma frequency. This aspect is more suitable to be addressed in a separate paper. The solution based on quasi-static formulation will first be presented. It will be seen that the predicted current flow in the spherical particle does not vary across the interior of the particle, even at very high charge concentration. The full-wave formulation is then presented, leading to a current distribution that becomes increasingly more confined to the surface of the particle as the charge concentration is increased.

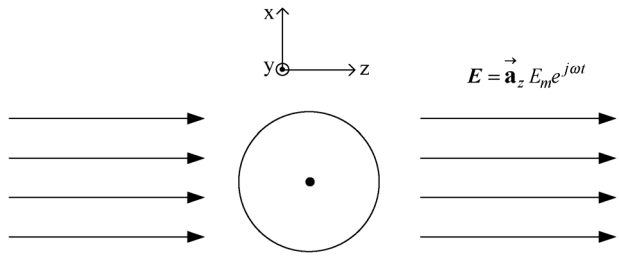


Fig. 1. Conductive sphere immersed in a dynamic electric field. Region outside the sphere is air.

## II. Theoretical Formulation

For a conductive sphere, as shown in Fig. 1, the distribution of the carriers inside it is governed by the Boltzmann's transport equation [21], [22] with corresponding force terms from coulombic interaction. The current density in the semiconductor sphere can be derived from the first order approximation to the Boltzmann's transport equation as

$$\frac{\partial(n\boldsymbol{v}_n)}{\partial t} = -\frac{kT}{m_n}\nabla n - \frac{qn}{m_n}\boldsymbol{E} - \frac{n\boldsymbol{v}_n}{\tau_n} \tag{1}$$

$$\boldsymbol{J}_n = -qn\boldsymbol{v}_n \tag{2}$$

$$\frac{\partial(p\boldsymbol{v}_p)}{\partial t} = -\frac{kT}{m_p}\nabla p + \frac{qp}{m_p}\boldsymbol{E} - \frac{p\boldsymbol{v}_p}{\tau_p} \tag{3}$$

$$\boldsymbol{J}_p = qp\boldsymbol{v}_p \tag{4}$$

$$\boldsymbol{J} = \boldsymbol{J}_n + \boldsymbol{J}_p \tag{5}$$

where $\boldsymbol{v}$, $m$ and $\tau$ are the velocity, the effective mass and the momentum relaxation time of the charge carriers ($n$ for electrons and $p$ for holes) respectively. $T$ is the absolute temperature and $k$ is the Boltzmann constant.

From (1) to (4), the free electron and hole current densities can be derived as

$$\boldsymbol{J}_n = q\mu_{ne}n\boldsymbol{E} + qD_{ne}\nabla n \tag{6}$$

$$\boldsymbol{J}_p = q\mu_{pe}p\boldsymbol{E} - qD_{pe}\nabla p \tag{7}$$

where

$$\mu_{ne} = \frac{\mu_n}{1+j\omega\tau_n} \qquad \mu_{pe} = \frac{\mu_p}{1+j\omega\tau_p}$$

$$D_{ne} = \frac{D_n}{1+j\omega\tau_n} \qquad D_{pe} = \frac{D_p}{1+j\omega\tau_p}$$

$$\frac{D_{ne}}{\mu_{ne}} = \frac{D_{pe}}{\mu_{pe}} = \frac{D_n}{\mu_n} = \frac{D_p}{\mu_p} = \frac{kT}{q} = \phi_T$$

$\mu_{ne}$, $\mu_n$, $\mu_{pe}$, and $\mu_p$ are the effective ac and dc mobility coefficient for free electrons and holes respectively and $D_{ne}$, $D_n$, $D_{pe}$ and $D_p$ are the effective ac and dc diffusion coefficients for free electrons and holes respectively. $\phi_T$ is the thermal voltage and is taken to be 0.0259 V.

Under the weak field assumption, (6) and (7) can be rewritten as

$$\boldsymbol{J}_n = q\mu_{ne}n_a\boldsymbol{E}_o + q\mu_{ne}n_o\boldsymbol{E}_a + qD_{ne}\nabla n_a \tag{8}$$

$$\boldsymbol{J}_p = q\mu_{pe}p_a\boldsymbol{E}_o + q\mu_{pe}p_o\boldsymbol{E}_a - qD_{pe}\nabla p_a \tag{9}$$

where $\boldsymbol{E}_o$ represents the static field and $\boldsymbol{E}_a$ represents the dynamic field. $n_o$, $n_a$, $p_o$, and $p_a$ are the mobile carriers (electrons and holes) for static and dynamic field component respectively.

When no static field is present, $\boldsymbol{E}_o = 0$, the equilibrium electron concentration $n_o$ and the hole concentration $p_o$ are determined by the doping levels, which is governed by the net impurity concentrations. Assuming n-type semiconductor with complete ionization, the ionized donor concentration $N_D \approx n_o$ and $p_o \approx n_i^2/n_o$. The current densities are given by

$$\boldsymbol{J}_n = q\mu_{ne} N_D \boldsymbol{E} + qD_{ne}\nabla n_a \tag{10}$$

$$\boldsymbol{J}_p = q\mu_{pe} p_o \boldsymbol{E} - qD_{pe}\nabla p_a. \tag{11}$$

The current continuity equation can be derived from the zero order moments of the Boltzmann's transport equation as

$$\nabla \cdot \boldsymbol{J}_n = q\frac{\partial n}{\partial t} + qR_n \tag{12}$$

$$R_n = \frac{n}{t_n} \tag{13}$$

$$\nabla \cdot \boldsymbol{J}_p = -q\frac{\partial p}{\partial t} - qR_p \tag{14}$$

$$R_p = \frac{p}{t_p} \tag{15}$$

where $R_n$ and $R_p$ are the electron and hole net recombination rates. These rates are related to the excess carrier densities and the corresponding lifetimes $t_n$ and $t_p$.

For an n-type semiconductor sphere, $N_D \gg N_A$ and $N_D \gg p$, so that $N_A$, $p_o$, and $p_a$ can be neglected for first-order analysis

$$\boldsymbol{J} = q\mu_{ne} N_D \boldsymbol{E} + qD_{ne}\nabla n_a \tag{16}$$

$$\nabla \cdot \boldsymbol{J} = q\frac{\partial n}{\partial t} + qR_n. \tag{17}$$

To be more general, we will use $N_e$ instead of $N_D$ in the following analysis, since electrons can be introduced by means other than doping. The electric field inside and outside of the sphere can be obtained with the wave equation

$$\nabla^2 \boldsymbol{E} + k^2 \boldsymbol{E} = \frac{\nabla \rho}{\varepsilon} + j\omega\mu\boldsymbol{J} \tag{18}$$

where $k^2 = \omega^2\varepsilon\mu$ is the wave number and $\rho$ is the charge density.

The boundary conditions at the surface of the sphere are

$$\boldsymbol{n} \cdot (\varepsilon_o \boldsymbol{E}^+ - \varepsilon_s \boldsymbol{E}^-) = 0 \tag{19}$$

$$\boldsymbol{n} \times (\boldsymbol{E}^+ - \boldsymbol{E}^-) = 0 \tag{20}$$

$$\boldsymbol{n} \cdot \boldsymbol{J} = 0 \tag{21}$$

where $\boldsymbol{E}^+$ represents the electric field in the air, $\boldsymbol{E}^-$ represent the electric field inside the sphere, and $\boldsymbol{n}$ is a unit vector normal to the boundary. This condition results from the inability of the charge carrier to move across the boundary formed by a conductor in contact with an insulator. In previous works on transport-field analysis for semiconductor interfaces, Neumann boundary condition was imposed on the current density due to the presence of junction effects [27]. The boundary condition in (21) bears the same spirit as the vanishing normal component of the electron fluid velocity at the surface, as applied to the analysis of a warm plasma sphere [28] but differs in the make up of the dielectric function. In the present study, the motion of the mobile charges is not combined with the electric displacement to form a complex dielectric function, but accounted for by a conduction current density which results from the action of the electric field and the concentration gradient of the mobile charges. The permittivity $\varepsilon_s$ in (19) includes only the effects of the lattice polarization involving the bound charges. The action of mobile charges is described by the electric current density, and subscribes to the boundary condition given by (21). In the presence of significant concentration gradient, screening of the electric field from the interior of a conductor becomes a dominant phenomenon that characterizes the dynamical properties of the charge-field interaction. The merits of employing a transport formulation to account for charge screening effect has been elaborated in a recent tutorial article [29]. The drift-diffusion formulation employed in the discussion to illustrate charge screening effects is equivalent to the transport equations for the charge carriers in this paper, as they all stem from the momentum relaxation approximation for the collision term in the Boltzmann's equation. The example given in [29] for the gold sphere made use of a complex local dielectric function, which incorporates the dynamics of the mobile charges, to give the boundary conditions for the electric displacement at the surface of the sphere. In the work presented in this paper, provision is made to keep track of the response of the bound charges and the mobile charges as separate quantities, thus allowing different boundary conditions to be specified for the displacement current and the conduction current at the surface of the sphere. At the same time, the added degrees of freedom in nonlocal permittivity functions [29] may be employed to account for non-uniform conductivity, including the boundary condition for the mobile charges at the surface of a conductor.

The above formulation can also be applied to metallic particles or particles containing ions as the conducting species[30], [31], provided the motion of the charge carriers can be described by the Boltzmann's equation with the momentum relaxation approximation. The appropriate parameters for the charge carriers, such as mass and relaxation time in the transport equations will need to be replaced, and the recombination rates should be set to zero.

## III. Basic Characteristics Of A Small Conductive Sphere Based on Quasi-Static Analysis

When the object being studied is much smaller than the wavelength, the fields can be considered as quasi-static. The quasi-static electric field has little retardation over the length scale of interest but is varying with time. Under the quasi-static assumption, the Poisson's equation can be applied to solve for the electric field

$$\nabla^2 \phi = -\frac{\rho}{\varepsilon_s} \tag{22}$$

$$\boldsymbol{E} = -\nabla\phi \tag{23}$$

$$\rho = -qn_a. \tag{24}$$

By applying the boundary conditions, the charge distribution and electric field are obtained as

$$\rho = -qA\left(\frac{\cosh(k_D r)}{k_D r} - \frac{\sinh(k_D r)}{k_D^2 r^2}\right)\cos\theta \tag{25}$$

$$\begin{aligned}\boldsymbol{E}^- = &\left\{-\frac{qA}{\varepsilon_s k_D^2}\left[\frac{2\sinh(k_D r)}{(k_D r)^2 r} + \frac{\sinh(k_D r)}{r}\right.\right.\\ &\left.\left. -\frac{2\cosh(k_D r)}{k_D r^2}\right]\cos\theta - C\cos\theta\right\}\hat{r}\\ &+\left\{\frac{qA}{\varepsilon_s k_D^2}\left[\frac{\cosh(k_D r)}{k_D r^2}\right.\right.\\ &\left.\left. -\frac{\sinh(k_D r)}{k_D^2 r^3}\right]\sin\theta + C\sin\theta\right\}\hat{\theta}\end{aligned} \tag{26}$$

$$\begin{aligned}\boldsymbol{E}^+ = &(E_a\cos\theta + 2Br^{-3}\cos\theta)\hat{r}\\ &+(-E_a\sin\theta + Br^{-3}\sin\theta)\hat{\theta}\end{aligned} \tag{27}$$

where the quantities $k_D$ and $L_D$ are given by

$$k_D^2 = \frac{\left[1 + \frac{\varepsilon_s(1+j\omega t_n)(1+j\omega\tau_n)}{qN_e\mu_n t_n}\right]}{L_D^2}$$

$$L_D = \sqrt{\frac{\varepsilon_s kT}{q^2 N_e}}$$

and the coefficient $A$, $B$, and $C$ are related by the boundary conditions, the applied external field and material properties

$$\begin{pmatrix} A \\ B \\ C \end{pmatrix} = \begin{pmatrix} \varepsilon_r\cdot F\cdot H & \frac{2}{a^3} & \varepsilon_r \\ \frac{F\cdot G}{a} & -\frac{1}{a^3} & 1 \\ -F\cdot H + \frac{\phi_T\cdot H}{N_e} & 0 & -1 \end{pmatrix}^{-1} \begin{pmatrix} -E_a \\ -E_a \\ 0 \end{pmatrix}$$

$$F = \frac{q}{\varepsilon_s k_D^2}$$

$$G = \frac{\cosh(k_D a)}{k_D a} - \frac{\sinh(k_D a)}{k_D^2 a^2}$$

$$H = \frac{2\sinh(k_D a)}{(k_D a)^2 a} + \frac{\sinh(k_D a)}{a} - \frac{2\cosh(k_D a)}{k_D a^2}.$$

The electric field, charge and current distributions for an n-type silicon semiconductor sphere with a radius of 0.5 $\mu$m and a doping level of $10^{16}$ cm$^{-3}$ and $10^{17}$ cm$^{-3}$ are shown in Fig. 2 to Fig. 4 when the external electrical field is 1.0 V/cm at $f = 10$ GHz. The semiconductor sphere has a relative permittivity $\varepsilon_r = 11.9$, electron mobility $\mu_n = 1500$ cm$^2$/V-s, electron momentum relaxation time $\tau_n = 2.156 \times 10^{-13}$ s, and electron life time $t_n = 0.0025$ s. Numerical simulation employing the COMSOL Multiphysics simulation tool is also performed to solve the system of equations. The numerical solutions were obtained by a finite element scheme applied to the grid points in the domain that subscribe to the relevant differential-integral equations. Fig. 5 illustrates the current distributions obtained by numerical method for an n-type silicon semiconductor sphere with a doping level of $10^{16}$ cm$^{-3}$.

There is no net charge inside the semiconductor sphere. When the electric field is applied, the electrons will move in a direction against the direction of the electric field, while the holes will move along the direction of the electric field. Since the hole concentration is low, the main contribution to the positive charge comes from the donor ions, which are immobile.

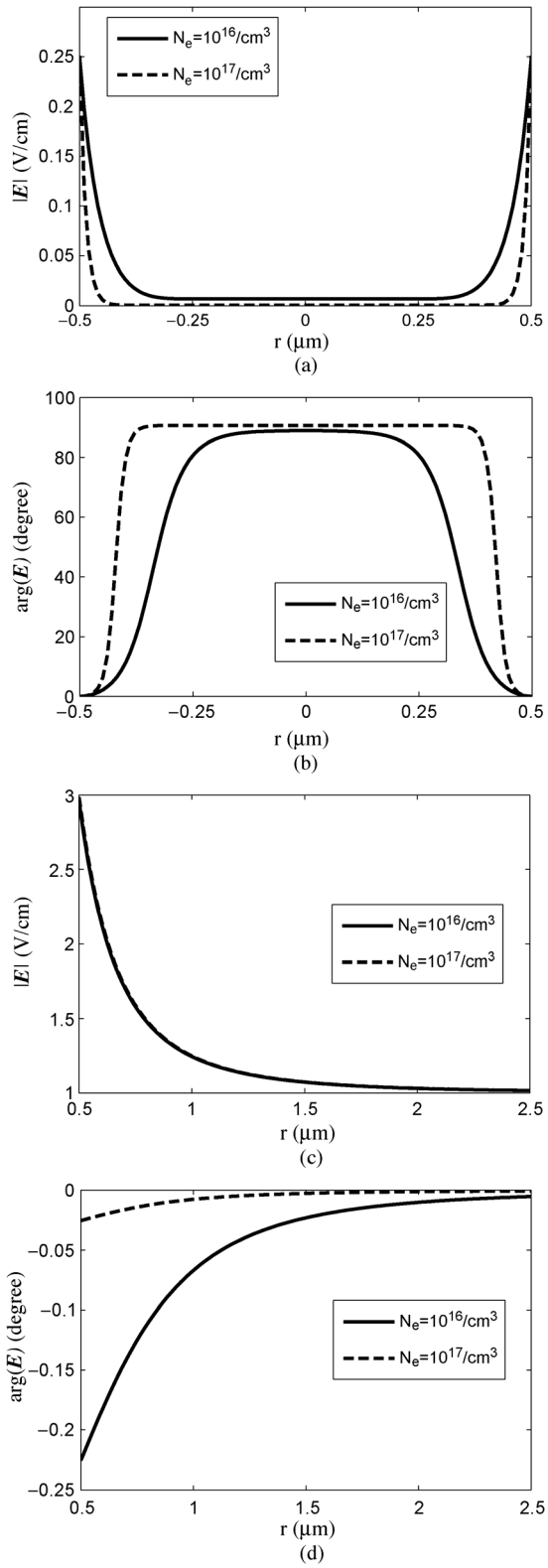


Fig. 2. Electric field along the $\hat{r}$ axis at $\theta = 0$ with $f = 10$ GHz. (a) Amplitude of electric field inside the sphere (b) Phase of the electric field inside the sphere. (c) Amplitude of electric field outside the sphere. (d) Phase of electric field outside the sphere.

A dipole moment is then induced by the applied external electric field. Fig. 6 shows the induced dipole moment versus frequency at different doping levels. It should be noted that the

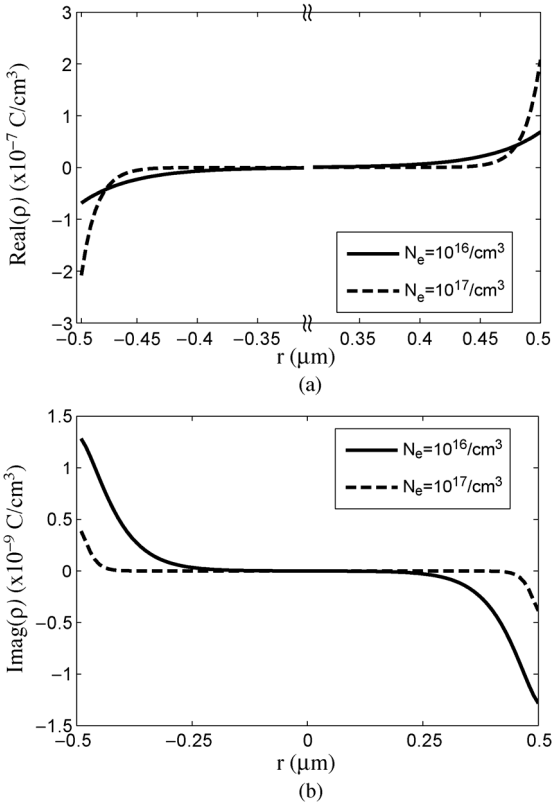


Fig. 3. Charge distribution inside the semiconductor sphere along the $\hat{r}$ axis at $\theta = 0$ with $f = 10$ GHz. (a) Real part. (b) Imaginary part.

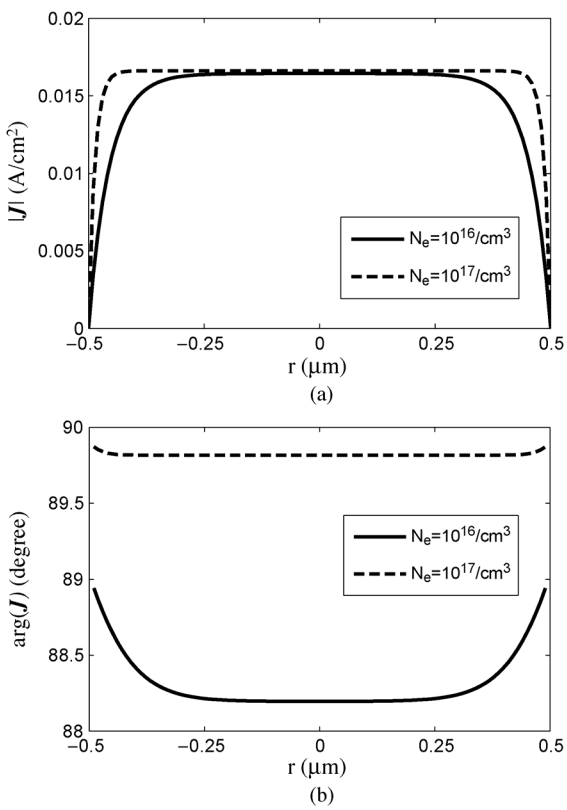


Fig. 4. Current distribution inside the semiconductor sphere along the $\hat{r}$ axis at $\theta = 0$ with $f = 10$ GHz. (a) Amplitude. (b) Phase.

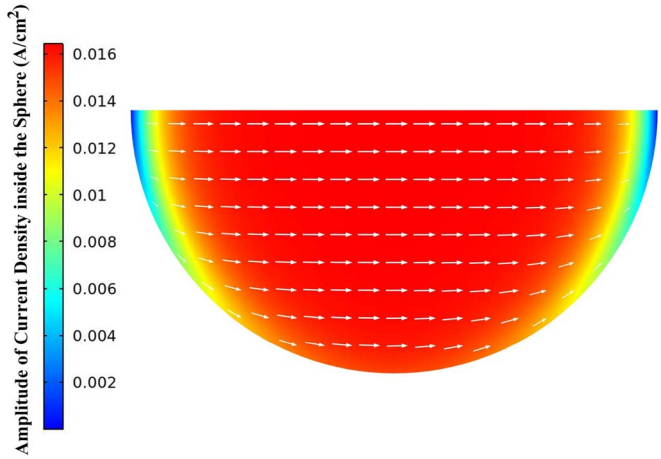


Fig. 5. Current distribution inside the semiconductor sphere with $N_e = 10^{16}$ cm$^{-3}$ obtained by numerical simulation.

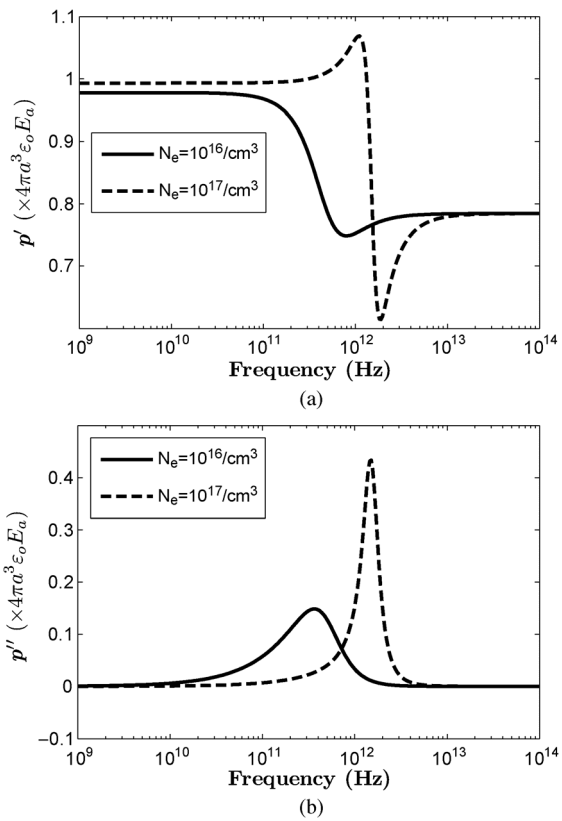


Fig. 6. Total induced dipole moment of the semiconductor sphere versus frequency. (a) Real part. (b) Imaginary part.

sign convention for the imaginary part of the dipole moment is defined according to $\boldsymbol{p} = \boldsymbol{p}' - j\boldsymbol{p}''$, which is different from the convention followed previously in [21]. As the doping level increases, the field is confined to the region close to the surface of the sphere, resulting in the real part of the dipole moment at low frequencies approaching that of a perfect electric conductor sphere immersed in a static field. The imaginary part of the induced dipole moment determines the power absorption by the semiconductor sphere. From Fig. 6(b), one can observe that

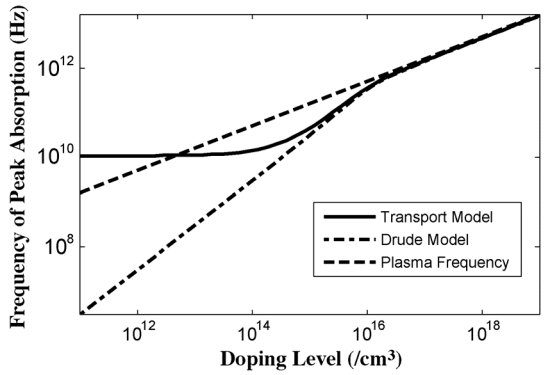


Fig. 7. Frequency of peak absorption versus doping level.

the absorption reaches its maximum at a certain frequency depending the doping level. We compare this peak absorption frequency with the plasma frequency at various doping levels in Fig. 7, with the plasma frequency defined by

$$\omega_{\text{plasma}} = \sqrt{\frac{N_e q^2}{\varepsilon_s m}} \tag{28}$$

The peak absorption frequency will approach the plasma frequency when the doping level is high, which follows from the physical meaning of the plasma frequency. The plasma frequency is the natural frequency of oscillation of electrons in a plasma displaced relative to the ion background. When there is a match in the excitation with the natural response of the charge interaction, the energy absorption reaches its maximum. The limitation of the quasi-static analysis is revealed when the current distribution is examined for the sphere with a high doping level. The magnitude of the current density at the center stays at a high level even for carrier concentration higher than $10^{20}$ cm$^{-3}$. This was checked against the solution obtained with a full-wave formulation and the difference between the two began to show when the carrier concentration exceeded $10^{20}$ cm$^{-3}$. The full-wave solution is described in the next section.

## IV. Full Wave Analysis

In most cases, when the object being studied is much smaller than the wavelength, the electric field inside this element is quasi-static. However the wavelength inside a conductive object will decrease as the carrier concentration increases and the quasi-static assumption will no longer be appropriate. Therefore, with a high doping level for a semiconductor sphere, the wave equation has to be utilized to solve for the electric field.

The wave equation in a semiconducting object can be obtained from (16), (17), and (18) as

$$\nabla^2 \boldsymbol{E} + k_s^2 \boldsymbol{E} = (j\omega\mu D_{ne} - \frac{1}{\varepsilon}) q \nabla n_a \tag{29}$$

where $k_s^2 = \omega^2 \varepsilon_s \mu - (j\omega\mu\sigma/(1+j\omega\tau_n))$, is the complex wave number

$$\sigma = q\mu_n N_e \tag{30}$$

$$jk_s = \alpha + j\beta = j\omega\sqrt{\varepsilon_s \mu}\sqrt{1 - j\frac{j\sigma}{(1+j\omega\tau_n)\varepsilon_s \omega}} \tag{31}$$

Hence, the wavelength in the semiconductor is given by $\beta$ as

$$\lambda_s = \frac{2\pi}{\beta} \tag{32}$$

By applying the boundary conditions, the charge distribution and the electric field can be obtained as

$$\begin{aligned}\rho \cong & -A' q \left( \frac{\cosh(k_D r)}{k_D r} - \frac{\sinh(k_D r)}{k_D^2 r^2} \right) \cos\theta \\ & + C' q \left( \frac{\cos(k_s r)}{k_s r} - \frac{\sin(k_s r)}{k_s^2 r^2} \right) \cos\theta \end{aligned} \tag{33}$$

$$\begin{aligned}\boldsymbol{E}^- \cong & \left\{ -\frac{qA'}{\varepsilon_s k_D^2} \left[ \frac{2\sinh(k_D r)}{(k_D r)^2 r} + \frac{\sinh(k_D r)}{r} - \frac{2\cosh(k_D r)}{k_D r^2} \right] \right. \\ & \left. + \frac{qC'}{\varepsilon_s k_s} \left[ \frac{\sin(k_s r)}{k_s r} \right] \right\} \cos\theta \hat{r} \\ & + \left\{ \frac{qA'}{\varepsilon_s k_D^2} \left[ \frac{\cosh(k_D r)}{k_D r^2} - \frac{\sinh(k_D r)}{(k_D r)^2 r} \right] \right. \\ & \left. - \frac{qC'}{\varepsilon_s k_s} \left[ \frac{\sin(k_s r)}{k_s r} \right] \right\} \sin\theta \hat{\theta} \end{aligned} \tag{34}$$

$$\begin{aligned}\boldsymbol{E}^+ = & (E_a \cos\theta + 2B' r^{-3} \cos\theta)\hat{r} \\ & + (-E_a \sin\theta + B' r^{-3} \sin\theta)\hat{\theta} \end{aligned} \tag{35}$$

where the constants $k_D$ and $L_D$ are given by

$$k_D^2 = \frac{\left[1 + \frac{\varepsilon_s (1+j\omega t_n)(1+j\omega\tau_n)}{q N_e \mu_n t_n}\right]}{L_D^2}$$

$$L_D = \sqrt{\frac{\varepsilon_s kT}{q^2 N_e}}$$

and the coefficient $A'$, $B'$ and $C'$ are related to the boundary conditions, the applied external field and material properties

$$\begin{bmatrix} A' \\ B' \\ C' \end{bmatrix} = \begin{bmatrix} \varepsilon_r \cdot F \cdot H & \frac{2}{a^3} & -\varepsilon_r \cdot M \\ \frac{F \cdot G}{a} & -\frac{1}{a^3} & -M \\ \varepsilon_r \cdot \frac{\phi_T \cdot H}{N_e} & \frac{2}{a^3} & -\varepsilon_r \cdot \frac{\phi_T \cdot N}{N_e} \end{bmatrix}^{-1} \begin{bmatrix} -E_a \\ -E_a \\ -E_a \end{bmatrix}$$

$$F = \frac{q}{\varepsilon_s k_D^2}$$

$$G = \frac{\cosh(k_D a)}{k_D a} - \frac{\sinh(k_D a)}{k_D^2 a^2}$$

$$H = \frac{2\sinh(k_D a)}{(k_D a)^2 a} + \frac{\sinh(k_D a)}{a} - \frac{2\cosh(k_D a)}{k_D a^2}$$

$$M = \frac{q\sin(k_s a)}{\varepsilon_s k_s^2 a}$$

$$N = -\frac{2\cos(k_s a)}{k_s a^2} + \frac{2\sin(k_s a)}{k_s^2 a^3} - \frac{\sin(k_s a)}{a}.$$

Equations (33) and (34) are approximate closed form expressions fitted to the full-wave simulation results. No exact closed form analytic expressions for the full-wave solution are available. By comparison of the full-wave numerical results obtained by simulation with the quasi-static solution, it was observed that the two agreed very well in the region within several Debye lengths from the surface but deviate from each other in the interior. In the interior, the solution can be constructed from a linear combination of the elementary solutions of the homogeneous form (forcing term set to zero) of (29). Hence in the region

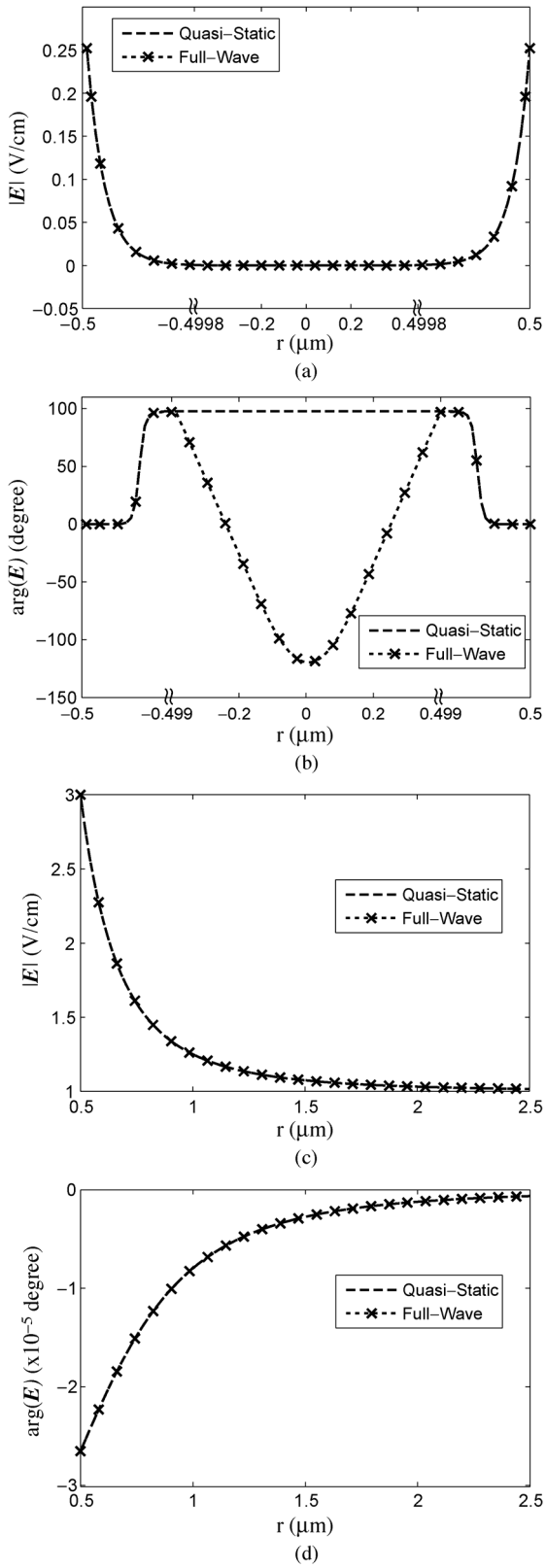


Fig. 8. Electric field distribution along the $\hat{r}$ axis at $\theta = 0$ with $f = 100$ GHz. (a) Amplitude of electric field inside the sphere. (b) Phase of the electric field inside the sphere. (c) Amplitude of electric field outside the sphere. (d) Phase of electric field outside the sphere.

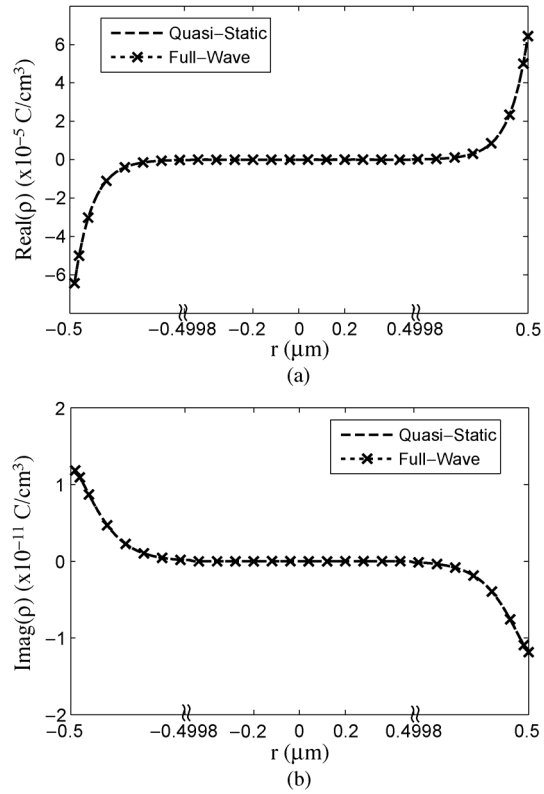


Fig. 9. Charge distribution inside the semiconductor sphere along the $\hat{r}$ axis at $\theta = 0$ with $f = 100$ GHz. (a) Real part. (b) Imaginary part.

where substantial charge accumulation can exist, the solution is essentially quasi-static, but in the rest of the space, propagation effects are significant. By superimposing the quasi-static solution with the full-wave solution, one can have closed form expressions for the solution that approximately track the results obtained by numerical simulation in the entire sphere. Equations (33) and (34) were obtained by this rationale and they give visually identical plots with the simulation results.

The electric field, charge and current distributions along the $\hat{r}$ axis at $\theta = 0$ for an n-type silicon semiconductor sphere with a radius of $0.5\mu$m and a doping level of $10^{22}$ cm$^{-3}$ are shown in Fig. 8 to Fig. 10. Although this level of doping may be exceeding the dopant solubility, its consideration can be justified from the theoretical stand point. For silicon the solubility for most dopants is less than $10^{21}$ cm$^{-3}$. Indeed, a carrier concentration of $10^{22}$ cm$^{-3}$ is approaching that of metals, but instead of carrying out the calculations with material parameters of a typical metal, we adhere to the same ones as those employed in the previous section for comparison purpose. The semiconductor sphere has a relative permittivity $\varepsilon_r = 11.9$, electron mobility $\mu_n = 1500$ cm$^2$/V-s, electron momentum relaxation time $\tau_n = 2.156 \times 10^{-13}$ s, and electron life time $t_n = 0.0025$ s. The external electrical field is 1.0 V/cm at $f = 100$ GHz. In these figures, the results from quasi-static analysis are also plotted for comparison. Fig. 11. shows the current distributions obtained by the numerical method.

Since the skin depth is much larger than the characteristic length, the screening effect is the dominant mechanism for preventing the external field from penetrating into the semiconductor sphere and one cannot find apparent deviations between the full wave and quasi-static analysis in the electric field and charge distribution near the surface, as shown in Fig. 8 and Fig. 9. However, due to the delay of the induced dipole moment

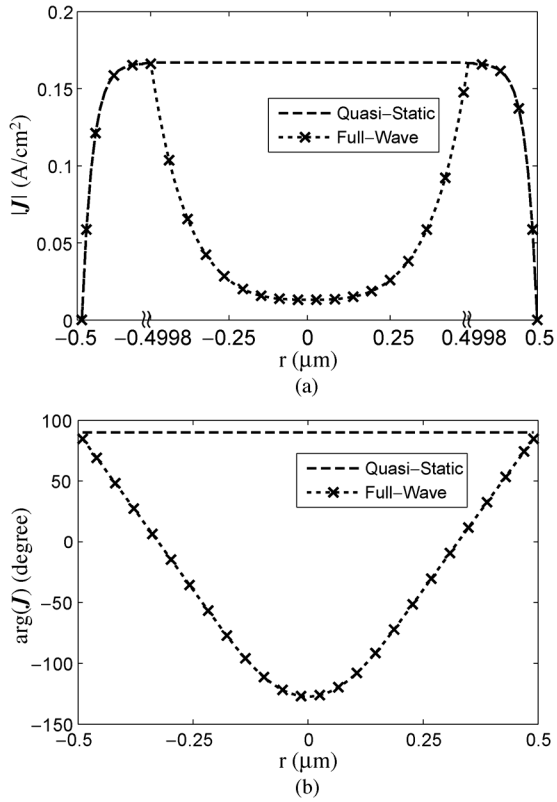


Fig. 10. Current density inside the semiconductor sphere along the $\hat{r}$ axis at $\theta = 0$ with $f = 100$ GHz. (a) Amplitude. (b) Phase.

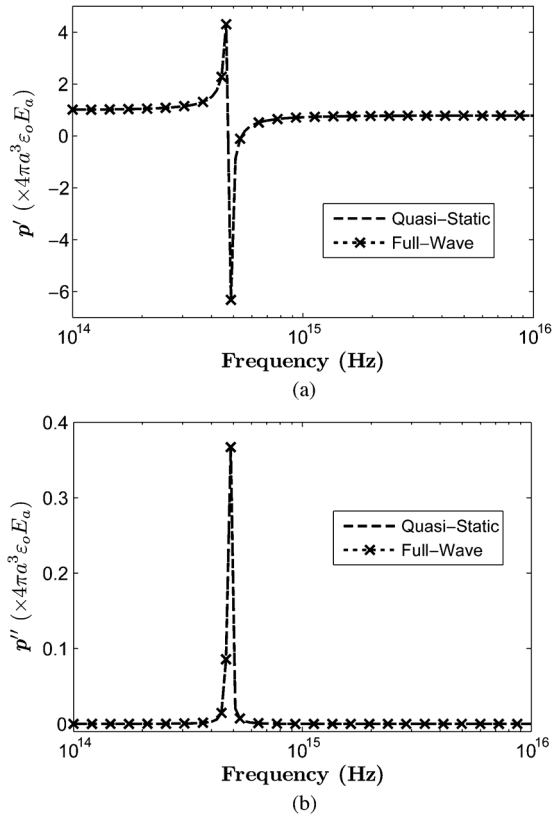


Fig. 12. Total induced dipole moment of the semiconductor sphere versus frequency. (a) Real part. (b) Imaginary part.

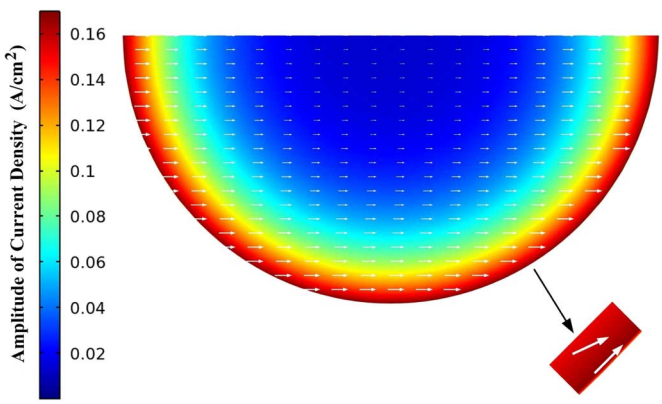


Fig. 11. Current distribution inside the semiconductor sphere with $N_e = 10^{22}$ cm$^{-3}$ obtained by numerical simulation.

relative to the applied electric field, the electric field can penetrate into the semiconductor object with a certain amplitude. This penetrating electric field is the key factor for the current distribution inside the semiconductor sphere though its amplitude is far below the field near the sphere surface. Therefore, the dissipation effect is the dominant mechanism for keeping the current distribution away from the center of the semiconductor sphere, as shown in Fig. 10. The result from full-wave analysis reveals that the current density shifts towards the region close to the spherical surface. This is also substantiated by the numerical result shown in Fig. 11. The current distribution is more confined to the surface as the doping level becoming higher. It is of interest to ponder why similar charge distributions arrived at by the quasi-static formulation and the full-wave formulation could lead to dissimilar current distributions when the charge concentration becomes high, as they are related by the continuity equation. In a time harmonic steady state, a given current distribution corresponds to a unique charge density function since the latter can be obtained with the divergence operator. However, a known charge density function in two or three dimensional space cannot guarantee a unique current distribution by consideration of the continuity equation alone. In one dimensional space, a given charge density function leads to a unique current distribution since the current density becomes a scalar and the continuity equation is sufficient to determine one from the other, apart from an additive constant. Fig. 8(c) and (d) shows the exterior field distribution and Fig. 12 illustrates the induced dipole moment versus frequency. The results from full-wave and quasi-static analyses show very little difference in the exterior field.

## V. Conclusion

The polarization within a conductive spherical particle induced by a dynamic electric field is investigated in terms of a transport model for the motion of the charge carriers, enabling the space charge effects to be revealed. By coupling the field equations to the transport equations of the charge carriers in a conductive particle, screening of the interior electric field by the polarized charges and the dynamics of the charge-field interaction are accounted for. Computation results for the case of an n-type semiconductor particle have been obtained to illustrate

the phenomena arising from the dynamics of the charge carriers induced by the applied electric field. For particles with carrier concentration lower than $10^{20}$ cm$^{-3}$, a quasi-static formulation based on the Poisson's equation coupled with the Boltzmann's equation with momentum relaxation approximation is employed, in which the conduction current and the displacement current are retained as separate variables, with specific boundary conditions to reflect the different constraints faced by the mobile charges and the bound charges at material interface. Very good agreement between analytic solution and numerical simulation are obtained. Frequency dependence of the total induced dipole moment displays strong dispersion and absorption near the bulk plasma frequency. Unlike the static case, there is a minute amount of interior electric field present in the sphere when the applied field is time dependent. The interior field is not completely screened as the polarization cannot follow instantaneously the applied field. This internal field is responsible for sustaining the current flow across the sphere. It is observed that quasi-static analysis is inadequate in addressing the internal charge interactions in a highly conductive sphere, even if its radius is much smaller than the free space wavelength. A full-wave formulation is needed to give a realistic account of the internal current distribution in a highly conductive particle. The full-wave formulation encompasses the full set of Maxwell's equations coupled with the Boltzmann's equation, along with the boundary conditions for the fields and charges at material interface. As the mobile charge concentration increases, the conduction current within the spherical particle becomes increasingly confined to the region close to the surface, and is adequately accounted for by the full-wave formulation but not by quasi-static analysis. The theoretical framework of charge-field interaction can be applied to other conductive objects made up of ionic conductors and metals provided the dynamics of the mobile charges can be described by the Boltzmann's equation with the momentum relaxation approximation, and the appropriate material parameters are substituted into the equations.

## REFERENCES


[1] J. J. Mock, D. R. Smith, and S. Schultz, "Local refractive index dependence of plasmon resonance spectra from individual nanoparticles," *Nano Lett.*, vol. 3, pp. 485–491, Mar. 2003.

[2] A. Alu and N. Engheta, "Polarizabilities and effective parameters for collections of spherical Nano-Particles formed by pairs of concentric double-negative (DNG), single-negative (SNG) and/or double-positive (DPS) metamaterial layers," *J. Appl. Phys.*, vol. 97, p. 094310, May 2005.

[3] G. W. Hanson, "Fundamental transmitting properties of carbon nanotube antennas," *IEEE Trans. Antennas Propag.*, vol. 53, no. 11, pp. 3426–3435, Nov. 2005.

[4] S. Arslanagic and R. Ziolkowski, "Active coated nanoparticles: Impact of plasmonic material choice," *Appl. Phys. A*, pp. 1–4, Jan. 2011.

[5] J. A. Stratton, *Electromagnetic Theory*. New York, NY, USA: McGraw-Hill, 1941.

[6] C. F. Bohren and A. J. Hunt, "Scattering of electromagnetic waves by a charged sphere," *Canad. J. Phys.*, vol. 55, pp. 1930–1935, Nov. 1977.

[7] P. W. Barber, J. F. Owen, and R. K. Chang, "Resonant scattering for characterization of axisymmetric dielectric sphere," *IEEE Trans. Antennas Propag.*, vol. AP-30, no. 3, pp. 168–172, Mar. 1982.

[8] E. Marx, "Electromagnetic pulse scattered by a sphere," *IEEE Trans. Antennas Propag.*, vol. 35, no. 4, pp. 412–417, Apr. 1987.

[9] M. S. Aly and T. T. Y. Wong, "Root nature of the transverse electric characteristic equation for a dissipative sphere," *IEEE Trans. Antennas Propag.*, vol. 37, pp. 71–77, 1989.

[10] M. S. Aly and T. T. Y. Wong, "Scattering of a transient electromagnetic wave by a dielectric sphere," *IEE Proc. H. Microw., Antennas, Propag.*, vol. 138, pp. 192–198, Apr. 1991.

[11] D. Worasawate, J. R. Mautz, and E. Arvas, "Electromagnetic resonances and Q factors of a chiral sphere," *IEEE Trans. Antennas Propag.*, vol. 52, no. 1, pp. 213–219, Jan. 2004.

[12] R. E. Kleinman, "The Rayleigh region," *Proc. IEEE.*, vol. 53, no. 8, pp. 848–856, Aug. 1965.

[13] J. D. Jackson, *Classical Electrodynamics*, 3rd ed. Hoboken, NJ, USA: Wiley, 1998.

[14] J. Richmond, "Scattering by a ferrite-coated conducting sphere," *IEEE Trans. Antennas Propag.*, vol. 35, no. 1, pp. 73–79, Jan. 1987.

[15] A. Lakhtakia and W. S. Weiglhofer, "Scattering by an electrically small bianisotropic sphere in a gyroelectromagnetic uniaxial medium," *IEE Proc. H. Microw., Antennas, Propag.*, vol. 139, pp. 217–220, Jun. 1992.

[16] F. Wu and K. W. Whites, "Quasi-Static effective permittivity of Periodic composites containing complex shaped dielectric particles," *IEEE Trans. Antennas Propag.*, vol. 49, no. 8, pp. 1174–1182, Aug. 2001.

[17] P. Debye, *Polar Molecules*. New York, NY, USA: Chemical Catalogue, 1929.

[18] G. Mie, "Beiträge zur Optik trüber Medien, speziell kolloidaler Metallösungen," *Ann. Phys.*, vol. 25, p. 377, 1908.

[19] M. Palandoken, A. Grede, and H. Henke, "Broadband microstrip antenna with left-handed metamaterials," *IEEE Trans. Antennas Propag.*, vol. 57, no. 2, pp. 331–337, Feb. 2009.

[20] A. Ishimaru, *Electromagnetic Wave Propagation, Radiation, and Scattering*. Upper Saddle River, NJ, USA: Prentice-Hall, 1991, p. 278.

[21] M. Yan and T. Wong, "Long wavelength polarization in a spherical particle containing mobile charge," in *Proc. IEEE AP-S Int. Symp.*, Albuquerque, NM, USA, Jul. 2006, pp. 935–938.

[22] C. Cercignani, *The Boltzmann's Equation and Its Application*. New York, NY, USA: Springer, 1987.

[23] K. Blotekjaer, "Transport equations for electrons in two-valley semiconductors," *IEEE Trans. Electron Devices*, vol. 17, no. 1, pp. 38–47, Jan. 1970.

[24] K. Han and T. T. Y. Wong, "Space-charge wave considerations in MIS waveguide analysis," *IEEE Trans. Microw. Theory Tech.*, vol. 39, no. 7, pp. 1126–1132, Jul. 1991.

[25] M. Yan and T. Wong, "Influence of charge dynamics on the internal field and current distribution in a conductive particle," in *Proc. URSI General Assembly*, Chicago, IL, USA, Aug. 2008, p. 310.

[26] M. Kerker, *The Scattering of Light and Other Electromagnetic Radiation*. New York, NY, USA: Academic, 1969.

[27] C. Krowne and G. Tait, "Propagation in layered biased semiconductor structures based on transport analysis," *IEEE Trans. Microw. Theory Tech.*, vol. 37, no. 4, pp. 711–722, Apr. 1989.

[28] R. Ruppin, "Plane wave interaction with a homogeneous warm plasma sphere," *Plasma Phys.*, vol. 17, pp. 723–730, 1975.

[29] G. Hanson, "Drift-diffusion: A model for teaching spatial-dispersion concepts and the importance of screening in nanoscale structures," *IEEE Antennas Propag. Mag.*, vol. 52, no. 10, pp. 198–207, Oct. 2010.

[30] D. Stein, M. Kruithof, and C. Dekker, "Surface-charge-governed ion transport in nanofluidic channels," *Phys. Rev. Lett.*, vol. 93, p. 035901, Jul. 2004.

[31] T. Shen, Z. Hu, and T. Wong, "Electric polarizability of a conductive nanoparticle and its equivalent circuit representation," in *Proc. IEEE AP-S Int. Symp.*, Orlando, FL, USA, Jul. 2013, paper no. 110.10.


**Tao Shen** received the B.S. degree from the University of Electronic Science and Technology of China (UESTC), Chengdu, China, in 2006, and the M.S. and Ph.D. degrees from the Illinois Institute of Technology (IIT), Chicago, IL, USA, in 2008 and 2013, respectively.

He was a teaching assistant in the Department of Electrical and Computer Engineering, IIT, from 2008 to 2011. From 2011 to 2012, he served as an Instructor in the Interprofessional Projects Program (IPRO), IIT. He was an engineering intern in the Analog and RF team of Mathworks, Inc., in 2009. He joined the Kunming University of Science and Technology, Kunming, China, as a Lecturer in 2012. His research interests include the space-charge interactions in nanostructures and systems, equivalent circuit modeling, and Terahertz measurement techniques.

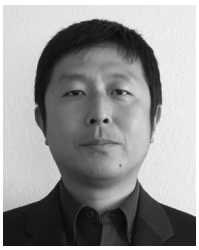

**Ming Yan** received his B.S. degree from Tsinghua University, Beijing, China, in 1999, and the M.S. and Ph.D. degrees from the Illinois Institute of Technology (IIT), Chicago, IL, USA, in 2002 and 2005, respectively.

He is currently an R&D Expert Engineer in Agilent Technologies. Prior to joining Agilent in 2006, he was a research assistant at the Microwave Laboratory of the Electrical and Computer Engineering Department, IIT, where he performed analysis on channel isolation in multi-carrier millimeter-wave communication systems and developed the framework for numerical simulation of charge interactions in nanostructures. His research interests include electromagnetic and semiconductor device modeling and broadband communication systems.

**Thomas T. Y. Wong** received the B.Sc. (Eng.) degree from the University of Hong Kong in 1975 and the M.S. and Ph.D. degrees from Northwestern University, Evanston, IL, USA, in 1978 and 1980, respectively.

From 1975 to 1976, he was a Product Engineer at Motorola Semiconductor (HK), Inc. At Northwestern University, he participated in establishing the Microwave Characterization Laboratory, where he carried out charge transport and dielectric property studies on ionic conductors, polymers and ceramics. He was a Research Fellow at the Materials Research Center in 1981. Since September 1981, he has been with the Illinois Institute of Technology (IIT), Chicago, IL, USA, where he is now a Professor in the Department of Electrical and Computer Engineering. He has conducted research in propagation effects on high-speed devices and integrated circuits, transient electromagnetics, material measurements, broadband millimeter-wave systems, and charge interactions in mesoscopic structures. In collaboration with Argonne National Laboratory and Fermilab, he has contributed to the development of dielectric-loaded accelerators, nanoscale motion sensors, and power couplers for superconducting cavity resonators. He is the author of *Fundamentals of Distributed Amplification* (Artech House) and co-author of *Electromagnetic Fields and Waves* (Higher Education Press). He is the originator of several issued patents on microwave electronics and wireless system design. He served as the Electrical and Computer Engineering Graduate Program Director at IIT from 1987 to 1995 and as the Chair of the Department of Electrical and Computer Engineering at IIT from 2001 to 2005. He was the Chair of the IIT faculty council in the 1998 academic year.

Dr. Wong served as the Chairman (1987–1988) of the IEEE Chicago Joint Chapter of AP-MTT Societies and has been a member of the organizing committees for several international technical conferences.